SMOS Wind Data Service

Readme First Note

Attention to: ESA

	Function	Name	Signature	Date
Prepared by	Consortium	IFREMER,ODL N.Reul, J. Tenerelli,JF Piolle		04/12/2023
Accepted by	ESA technical officer	Raffaele Crapolicchio	Raffaele Crapolicchio	04.12.2023

Laboratoire d'Océanographie Physique et Spatiale – Z.I. Pointe du Diable-B. P. 70, Plouzané – France
Tél. : +33 (0)2 98 22 44 10 – Fax : +33 (0)2. 98. 22. 45. 33 – E-mail : nreul@ifremer.fr

Indexing form

Customer	ESA/ESRIN	**Contract N°4000122821/17/I-EF**				
Confidentiality codes				**Document management**		
Company / Programme		Defence				
Non-protected ☐		Non-protected ☒		None ☐		
Reserved ☒		Limited diffusion ☐		Internal ☒		
Confidential ☐		Defence confidentiality ☐		Customer ☐		
Contractual document		**Project N°**		**Work Package**		
Yes ☒ No ☐				-		
Readme First Note						
Summary						
SMOS wind products Readme First Note						
Document						
File name	SMOS_WIND_RM_TN_v2.3_20230522			Nbr of pages	28	
Project	-			Nbr of tables	0	
Software	Microsoft Office Word			Nbr of figures	0	
Language	English			Nbr of appendices	0	
Document reference						
Internal				Issue 2	Date	
External				Revision 3	Date	22/05/2023
Author(s)		**Verified by**		**Authorised by**		
Nicolas REUL		JF Piolle		Nicolas Reul		

Laboratoire d'Océanographie Physique et Spatiale – Z.I. Pointe du Diable-B. P. 70, Plouzané – France
Tél. : +33 (0)2 98 22 44 10 – Fax : +33 (0)2. 98. 22. 45. 33 – E-mail : nreul@ifremer.fr

Distribution list

INTERNAL	EXTERNAL	
Name	**Name**	**Company / Organisation**
N. REUL J.TENERELLI S. HERLEDAN J-F. PIOLLE C. LE JEUNE D. BRIAND	R. CRAPOLICCHIO	ESA

Document status

Title			
SMOS wind data service readme first note			
Issue	**Revision**	**Date**	**Reason for the revision**
1	0	04/02/2020	Initial version
1	1	04/03/2020	RC comments from the 05/02/2020 + change of the http access to the password from the Ifremer dissemination service
2	0	01/07/2021	Update for the new L1 and Wind retrieval processor
2	1	04/08/2021	RC comments for final document delivery
2	2	20/10/2022	DB adds section 2.3 : Minor Update for v302
2	3	22/05/2023	DB adds section 2.4 : Minor Update for v303
2	4	22/11/2023	DB adds section 2.4 and 2.5 : Minor Updates for v304 and v305

Modification status				
Issue	Rev	Status *	Modified pages	Reason for the modification
2	2	I	15	New version of the products (v302)
2	3	I	16	New version of the products (v303)
2	3	I	17	New version of the products (v304/v305)

* *I = Inserted* *D = deleted* *M = Modified*

Table of contents

1. Introduction

1.1. Scope and structure of the document

This “Readme first” note provides to the SMOS NRT Wind Data Service users:

- An overview of the SMOS wind products version 305 content, a description of the algorithm evolution implemented and a summary of the products validation results (§2),
- The way to access the data through both Ifremer FTP/HTTP and the ESA/SMOS dissemination portal (§3),
- The way to access SMOS wind product documentation (§4).
- A reference to scientific publications (§5).

1.2. Applicable and Reference Documents

1.2.1. Applicable Documents (ADs)

The following is the list of applicable documents:

Table-1: SMOS Wind Data Service Applicable Documents

Ref.	Title	Code	Version	Date
[AD.1]	SMOS NRT Product Format Specification Document	SO-ID-DMS-GS-0002	4.2	25.03.2019
[AD.2]	SMOS Wind Data Service Algorithm Theoretical Basis Document	SMOS_WIND_DS_ATBD.docx	1. rev 5	04.08.2021
[AD.3]	SMOS Wind Data Service Product Description Document	SMOS_WIND_DS_PDD.docx	1. Rev 6	04.08.2021
[AD.4]	SMOS Wind Products First Reprocessing Plan	TN_SMOS_WIND_DS_ORR_TRR.docx	1. Rev1	23.10.2019
[AD.5]	Read-me-first note for the release of the SMOS Level 1 data products	https://earth.esa.int/eogateway/documents/20142/37627/Read-me-first-note-for-the-release-of-the-SMOS-Level-1-data-products		25 May 2021

1.2.2. Reference Documents (RDs)

The following is the list of reference documents:

Table-2: SMOS Wind Data Service Reference Documents

Ref.	Title	Code	Version	Date
[RD.1]	Sampson, C. R., and A. J. Schrader, The Automated Tropical Cyclone Forecasting System (version 3.2).	Bull. Amer. Meteor. Soc., 81, 1231–1240	n/a	2000
[RD.2]	Bourassa, M. and co-authors. Remotely Sensed Winds and Wind Stresses for Marine Forecasting and Ocean Modeling	Frontiers In Marine Science , 6(443), 28p.	n/a	2019

1.3 Acronyms and Abbreviations

AMSR-2	Advanced Microwave Scanning Radiometer 2
ATBD	Algorithm Theoretical Baseline Document
ATCF	NOAA Automated Tropical Cyclone Forecast system
BTs	Brightness Temperature
GMF	Geophysical Model Function
IFREMER	Institut Francais de Recherche pour l'Exploitation de la Mer
MIRAS	Microwave Imaging Radiometer using Aperture Synthesis
NOAA	National Oceanic and Atmospheric Administration
NRT	Near Real Time
ODL	Ocean Data Lab
PDF	Probability Distribution Function
QL	Quality Level
RFI	Radio Frequency Interference
RMS	Root Mean Square
SMAP	Soil Moisture Active Passive
SMOS	Soil Moisture and Ocean Salinity ESA's EO mission
SWS	Surface Wind Speed
TC	Tropical Cyclone

2. SMOS Wind Data Service Products and Validation

2.1. SMOS wind Data Service Products

As described in [AD.3], the SMOS wind Data Service produces **3 types of products**:

1. **"SMOS Near Real Time Level 2 swath wind speed" (SMOS L2WS NRT) products**, which are SMOS retrieved surface wind speed gridded maps with a spatial sampling of 1/4°x 1/4° and consisting of orbital segments (containing parts of ascending and descending half orbits) following the granularity of the SMOS Level 1B near real time (NRT) data products [AD.1]. SMOS L2WS NRT products are available within 4 to 6 hours from sensing and are generated in NetCDF-4 format as described in [AD.3]**.**

2. **SMOS "wind radii fixes" (SMOS WRF) products**. Using the Tropical Cyclones (TCs) best-track storm center and intensity forecasts from the Automated Tropical Cyclone Forecast System (ATCF) developed by Naval Research Laboratory, Marine Meteorology Division [RD.1], SMOS L2 swath which intercepts current storms are determined. For interceptions with sufficient swath coverage, the processor produces SMOS WRF files generated in the so-called "Fix (F-deck)" ATCF format. The SMOS WRF "fixes" to the best-track forecasts contain: the SMOS 10-min maximum-sustained winds (in knots) and wind radii (in nautical miles) for the 34 kt (17 m/s), 50 kt (25 m/s), and 64 kt (33 m/s) winds per geographical storm quadrants and for each SMOS pass intercepting a TC in all the active ocean basins. SMOS WRF products are available within 4 to 6 hours from sensing and are generated in ASCII format as described in in [AD.3]. **N.B. since product version 300 a three-digit file counter has been added to the wind radii fixes filename.**

3. the **"SMOS Level 3 daily wind speed" (SMOS L3WS) products.** SMOS L3WS products are daily composite maps of the collected SMOS L2 swath wind products for a specific day, provided with the same grid than the Level 2 wind data (SMOS L2WS NRT) but separated into ascending and descending passes. SMOS L3WS products are available the day after from sensing and are generated in NetCDF-4 format as described in [AD.3].

2.2. Major processing changes from previous processor version

Several updates of the SMOS NRT L2 wind processor V300 baseline have been applied to account for:

1) the new version of the SMOS brightness temperature L1B products (v724) which are now used as input to the SMOS wind processor (see [AD.5])

2) A new SMOS wind retrieval method based on a Bayesian retrieval algorithm (see details in §3.6 of [AD.2]),

3) The correction of small bugs found in some of the forward model corrections,

4) changes in some of the auxiliary geophysical data used for the retrieval.

These changes are summarized hereafter:

1.1.1. Support for Level 1B products version v700+ with Gibbs-2 image reconstruction.

The Land Sea Contamination (LSC) correction lookup table file has been updated to account for the new L1B version v724.

After computing the Brightness Temperature from the frequency components, the extended sources that may have been subtracted during L1b processing, in order to perform Gibbs error mitigation, have to be added back. Depending on the Gibbs level it can be a constant flat Earth (Gibbs=1), or a constant flat Land plus a model Ocean (Gibbs=2). The flat Earth or Land values are annotated in the L1b product, whereas the Ocean model is the same. The discrimination between Land and Ocean in order to add back the constant Land or the model Ocean for Gibbs 2 baseline is done based on the pixel water fraction content, considering it as Land if the water fraction is below 50% and Ocean if it is above or equal to 50%. The two Gibbs options and the Artificial Scene Library have been added and implemented into the L1B processing of the SWS wind processor.

1.1.2. Fix of product dates when no valid retrievals exist in products.

A bug was found for some SMOS NRT L2 wind products version 110 which had "no wind values". This was related to the netCDF file which had erroneously wrong start and stop time. The dates in the SMOS NRT L2 wind products are now the dates of the L1B files and this problem is fixed.

1.1.3. Fix of the sun glint calculation

At the surface, the brightness temperature of the scattered solar radiation in polarization *p* may be expressed as (Reul et al., 2007 [RD.14]):

$$T_{ssp} = (\tau_d \tau_v) \frac{\overline{T}_{sun}(t)\Omega_{sun}}{4\pi cos(\theta_s)} \left[\sigma_{pp}(\theta_o, \phi_o, \theta_s, \phi_s) + \sigma_{pq}(\theta_o, \phi_o, \theta_s, \phi_s)\right]$$

where $\overline{T}_{sun}(t)$ is the brightness temperature of the sun averaged over the solar disc at 1.4 GHz and at time *t*, Ω_{sun}=8.2 x 10^{-5} sr is the solid angle of the sun at L-band, *p* and *q* represent the polarizations H or V, and $(\sigma_{pp}, \sigma_{pq})$ are the bistatic scattering cross-sections of the rough sea surface, expressed as functions of the scattering geometry. The incidence and azimuth angles from the scattering surface toward the sun are θ_o and ϕ_o, respectively, and the corresponding angles towards the satellite are θ_s and ϕ_s. Atmospheric attenuation on the downward path from the sun to the sea surface is accounted for by the factor $\tau_d\tau_v$.

In the old wind processor v110, there was a bug in the angle used in the denominator $cos(\theta_s)$of the above equation: the incidence angle θ_o was used instead of the scattered angle θ_s. This problem was found during cross-validation of the sun glint model with Ali Khazaal and has the effect of overcorrecting for the sun glint. As found (Figure 1), the fresh bias observed between model and observation on the right side of the swath in winter descending passes is now significantly reduced.

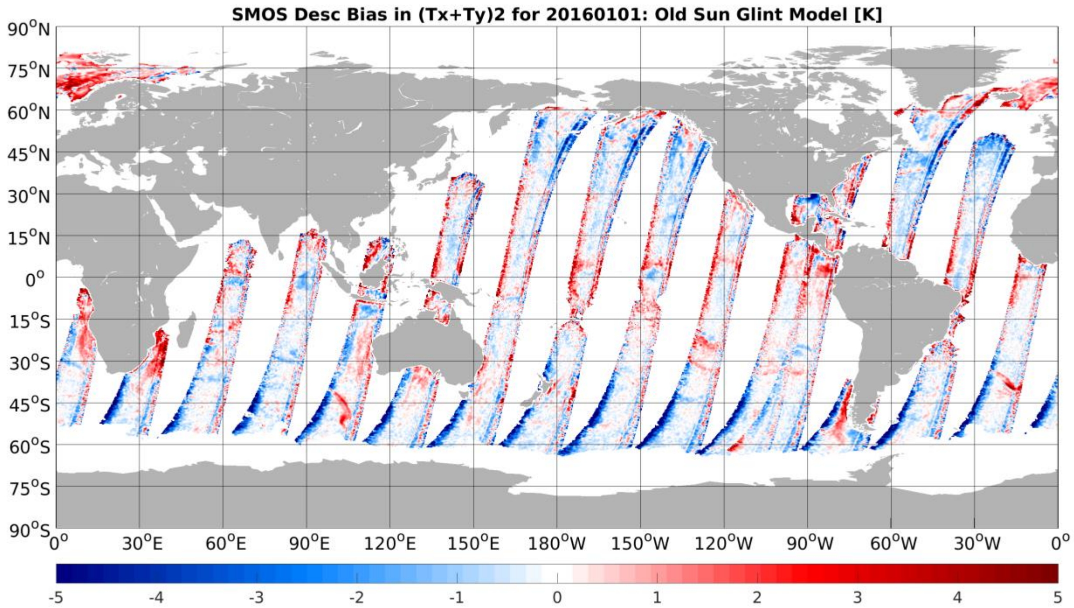

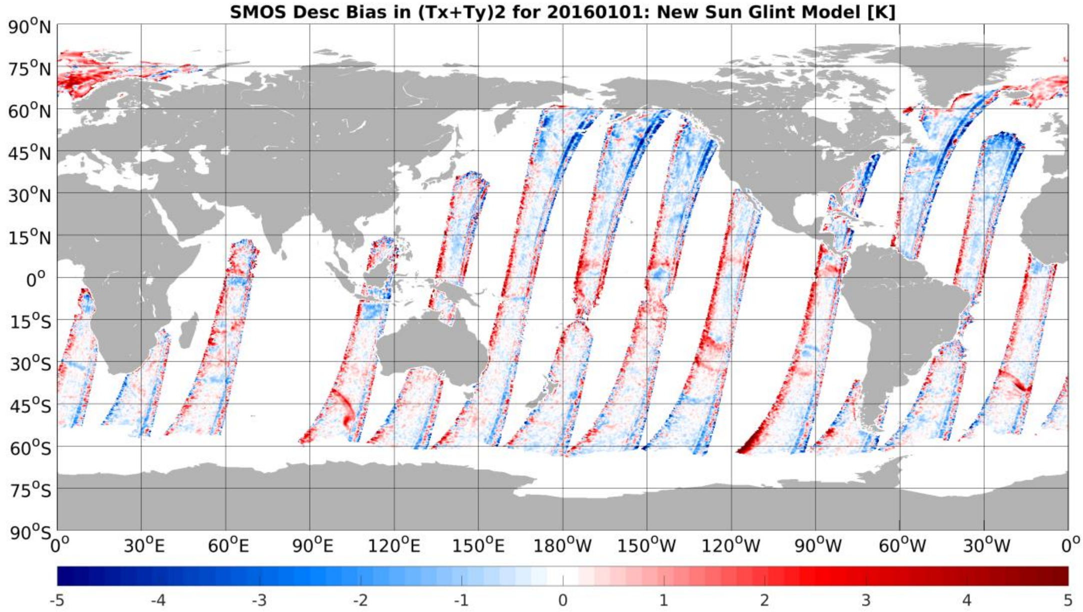

Figure 1 : Impact of changing the angle on the sunglint correction bug. Top: old correction for products version 110. Bottom: new correction for products version 300.

1.1.4. Addition of option for use of the CCI SSS as reference SSS fields.

To correct for the flat ocean surface emission, the processor can now use as the reference SSS fields, the ESA/CCI SSS L4 daily, 25 km resolution product.

The products are available at https://climate.esa.int/en/projects/sea-surface-salinity/

These improved quality auxiliary satellite SSS are only used for the SMOS wind data reprocessing version 300. For the operational processor, we still rely on the CMEMS operational SSS forecasts fields.

1.1.5. Addition of the new model of sea water dielectric constant of Boutin-Vergely

To estimate the specular emission, the processor now apply the new sea water dielectric constant model at L-band developed by Boutin et al. (2020).

Boutin Jacqueline, Vergely Jean-Luc, Dinnat Emmanuel P., Waldteufel Philippe, D'Amico Francesco, Reul Nicolas, Supply Alexandre, Thouvenin-Masson Clovis Correcting Sea Surface Temperature Spurious Effects in Salinity Retrieved From Spaceborne L-Band Radiometer Measurements . *IEEE Transactions on Geoscience and Remote Sensing* IN PRESS . Publisher's official version : https://doi.org/10.1109/TGRS.2020.3030488

1.1.6. Addition of the new galactic glint model.

New celestial sky glint model has been developed and documented in the frame of the L2OS project. Largest differences with respect to old model occur at low wind speeds. In the empirical models (even the new one) the glint solutions for wind speeds between 0 m/s and the lowest model wind speed (3 m/s) are weighted combinations of the specular and lowest nonzero wind speed solutions. In the old model, the lowest wind speed for which a rough surface solution exists is 3 m/s. Thus, for wind speeds below 3 m/s the solution is ramped to the (synthetic beam averaged) specular glint solution at 0 m/s. This leads to some residual bias at low wind speeds. For the new model, the slope distribution is expanded in a series of Gaussian distributions. The reader will find details in the updated ATBD [AD.2].

1.1.7. Addition of auxiliary file (rather than RSGA) option for solar flux for sun glint calculation.

Different sources for solar flux can now be used by the processor: RedLab/SERCO rescaled Solar flux from radio-telescope measurements have been added to complement the first source which was RSGA.

1.1.8. Change in the data filtering around the direct sun aliases:

The disc within which all Brightness Temperatures (Tbs) are removed around the sun and sun alias images was expanded from 0.05 to 0.2 antenna frame's director cosine units, but only for wind speed retrievals (not for OTT calculation). Indeed one can still see along-track streaks in descending passes in December/January, even with this larger disc radius of 0.2 which is quite large. A new option has also been added to filter out measurements within some distance of the sun tails, but the streaks remain even with this option.

1.1.9. Option to use a scattering cross section file with no negative cross sections.

Some small negative values appear in the Sky glint forward model Look Up Tables due to difficult numerical integration (diffraction integral) issues at large incidence angles. An option to use a scattering cross section LUT in which all negative cross sections have been set to zero has been added. This makes only a slight (0.01 K) difference in swath biases.

1.1.10. Tb filtering based on distance to primary sun alias tails

We added L1B Tb filtering using distance from primary sun alias tails (tails associated with the sun alias inside the fundamental hexagon). To use this tail filter, we added a filter parameter which if equal to 0.2 dcu, then it will remove all Tbs within 0.2 dcu from the primary sun alias tails.

1.1.11. Use of a Bayesian wind speed retrieval.

In the non-bayesian retrieval method, the first Stokes parameters of the difference between the OTT-corrected MIRAS brightness temperatures and those of the forward model (without rough surface emission included) are averaged over the earth dwell lines to produce a map of

dwell-line averaged rough surface excess emission first Stokes parameter. The brightness temperatures entering the averaging are weighted by the inverse of the variance of the MIRAS Tbs, which is taken to be an isotropic function of distance from boresight in director cosine coordinates.

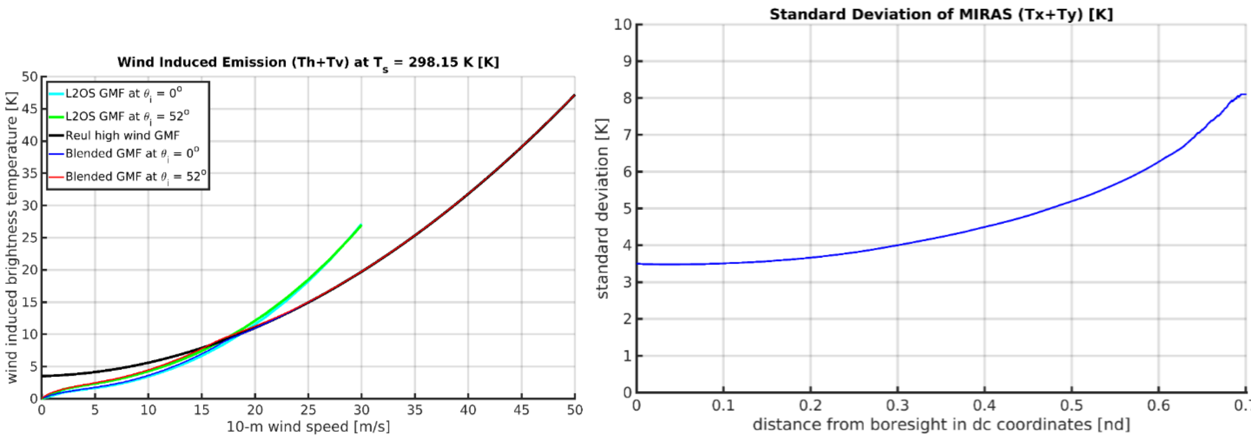

Figure 2 : (Top) square root of the variance of the MIRAS Tbs as a function of distance from boresight in director cosine coordinates. (Bottom) Wind GMF used by the processor

The square root of this variance function is shown in Figure 2. The GMF in the form of wind speed as a function of the average (incidence angle independent) rough surface excess emission to 10-m wind speed is then used to map the residuals to wind speed.

In the Bayesian method, Bayes' Theorem is used to express the PDF of the (unknown) retrieved wind speed as the product of the PDF of the measurements (for any given dwell line) given the wind speed and the prior distribution of the wind speed (independent of the measurements and given by ECMWF forecast fields). The PDF of the measurements is computed by assuming that each measured first Stokes parameter is a sample from a Gaussian distribution with a maximum at the model prediction for any wind speed and with a variance given by the function in Figure 2.

The individual Gaussian distributions for all nonfiltered measurements for a given dwell line are multiplied to produce the likelihood function for that dwell line. This likelihood is then multiplied by the prior wind speed distribution to produce the posterior PDF of retrieved wind speed. From this posterior PDF three point estimates of the retrieved wind speed are produced (mean, median and mode) along with second third and fourth central moments. The second central moment is used to provide an estimate of the standard deviation of the retrieved wind speed. The model solutions used to compute the likelihood functions employ the same GMF as used in the non-bayesian method, but expressed as excess roughness emission as a function of wind speed (the inverse of the function used in the non-Bayesian method). This GMF is shown in Figure 2 along with the Reul HWS GMF and the Level 2 OS GMF for low wind speeds.

The prior PDF of the wind speed takes the form of a Rice distribution. This distribution is appropriate as a wind speed distribution if the speed corresponds to individual orthogonal wind vector components that are both Gaussian distributed with the same variance. This prior PDF is formulated as a function of two hyper-parameters the wind speed at the peak of the distribution and the standard deviation of the corresponding wind components.

The wind speed at the peak is set equal to the ECMWF 10-m neutral equivalent wind speed, and the component standard deviation is a linear function of the equally-weighted average of the (unknown) retrieved wind speed and the ECMWF wind speed, with a slope of 0.2. The component standard deviation at zero wind speed is set equal to 0.1 m/s.

The reader will find details in the updated ATBD [AD.2].

1.1.12. Change in the calculation of the quality level:

Previous products version 110 contained a bug in which the quality level was erroneously set to 2 rather than 1 for gridpoints with across-track distance exceeding 250 km. This has been changed.

1.1.13. Changes in the calculation of wind radii:

The minimum non-missing value count at each radius is now 30% of the total. Before it was set to 50%.

2.3. Minor update v302

A minor update (v302) was put into operation in order to remove bad values.

In this version some previously ignored flags are taken into account : the 302 version does not use scenes for which any of the associated snapshots (XX, YY, Re(XY), Im(XY)) contain a nonzero value for at least one of the following flags in the L1B product:

- Calibration_Error_flag
- Software_Error_flag
- Instrument_Error_flag
- ADF_Error_flag

Furthermore, any scene for which antenna boresight incidence angle is outside the range [34,41] degrees is not used for wind retrieval. In the previous versions of the processor this range check was only applied for OTT creation and not for the wind product generation.

2.4. Minor update v303

A minor update (v303) was put into operation in order to cope with the format evolution of the Copernicus Marine Service product "GLOBAL_ANALYSISFORECAST_PHY_001_024" used in the processing chain.

2.5. Minor update v304

A minor update (v304) was put into operation from 10 November 2023 until 17 of November in order to take into account measurements with the instrument error flag raised. It has been observed that during this period many ocean measurements have been flagged with this error and that this is mostly associated with receiver physical temperatures in Arm A exceeding 29°C. This does not impact the quality of the wind retrievals, but these measurements were nonetheless ignored by the previous version of the wind processor. This new version ignores the instrument error flag and incorporates the flagged data in the wind retrieval.

2.6. Minor update v305

A minor update (v305) was put into operation in order to improve the solar flux used in the sun glint correction. Previously, daily 10.7 cm fluxes measured at the Penticton observatory (as provided in the NOAA/USAF RSGA reports) were used to estimate the L-band flux for the glint calculation. With this update the solar flux is obtained from SMOS measurements itself with a latency of one day.

2.7. SMOS NRT wind product version 300 baseline summary of the validation results

We compared SMOS SWS retrieved with the new processor version 300 with SMAP data for 4 months (August and September 2015 and 2019) and inter-compared the results with those found for the previously operated processor version 110 (hereafter referred to as the "Old processor").

1. The old processor version 110 was generating SMOS winds with erroneous wind speed Probability Distribution Function (PDF) in the low wind speed regimes (see Figure 3). Problems at low winds (such as strange peaks in the PDF at SWS~2 m/s) are no more observed with the new processor using the Bayesian inversion, which solved the erroneous SMOS wind PDF distribution. SMOS wind 's PDF now well matches the SMAP ones whatever the SMOS wind Quality level values.

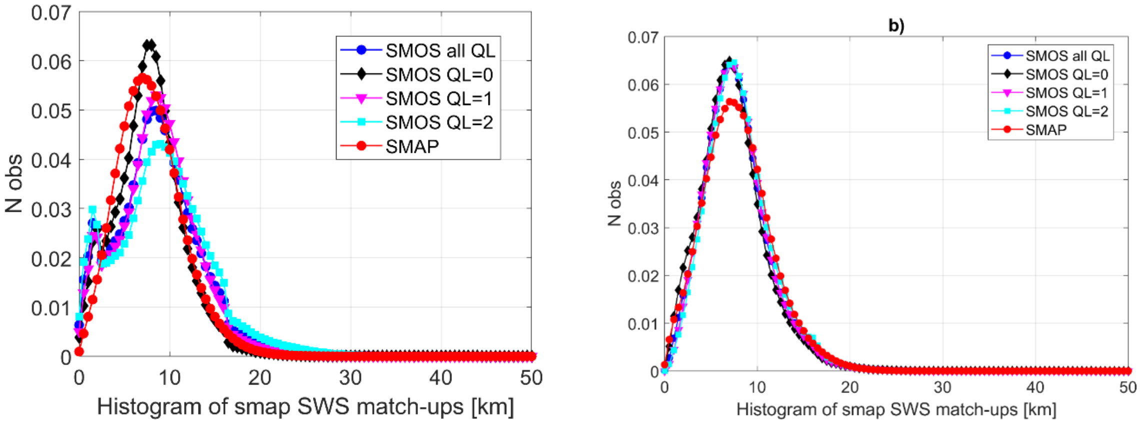

Figure 3 : Probability Distribution Function (PDF) of the retrieved wind speed for SMOS NRT wind (blue) and SMAP (red) wind considering all the SMOS/SMAP match-ups. SWS' PDF for SMOS data with QL=0 (black curve), QL=1 (magenta) and QL=2 (cyan) are also shown. Left: Old processor v110. Right: New Processor v300.

2. The **RMSD between SMOS and SMAP is** strongly reduced by about a factor 2 with the new processor **reaching 1.9 m/s for all QL values**. It reaches 1.7 m/s for QL=0 (see Figure 4).

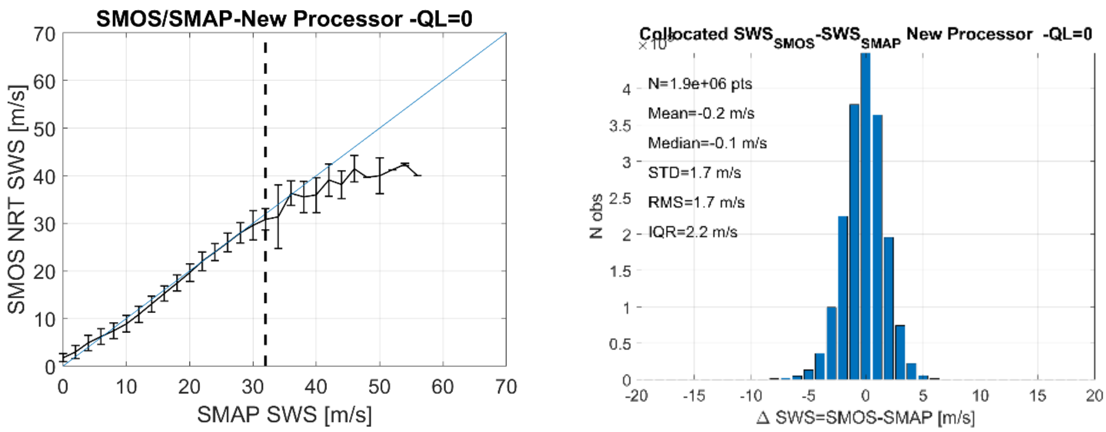

Figure 4 : (Left) Bin-averaged SMOS NRT retrieved surface wind speed as function of SMAP retrieved surface wind speed for co-located pairs (within 25 km, ±1 hour) in August and September 2015 & 2019. The vertical bars show ±1 standard deviation per 2 ms-1 bin-width. (right) Histogram of the surface wind speed differences between SMOS and SMAP at co-localized match-up pairs. Only SMOS NRT data with Quality Level =0 (good) are accounted for.

3. As found for all wind speed ranges, STD and RMSD between SMOS and SMAP decrease significantly with the new processor version 300. **SMOS winds are still however systematically lower than SMAP in hurricane wind conditions (> 32 m/s)**. The bias increases with increasing wind speed, reaching about 5-10 m/s at 50 m/s.

4. As found, STD and RMSD between SMOS and SMAP wind speed **decrease significantly with the new processor as function of across-track distance from the central part of the swath** (see Figure 5). Strong biases & increased RMSD found on the border of the swath with the old processor have vanished in the new processor. The RMSD is still little higher in the central part of the swath for QL=2.

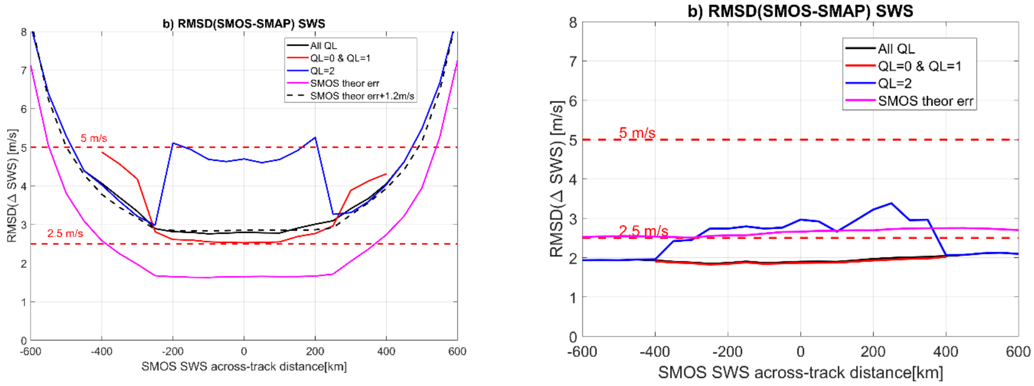

Figure 5 : RMSD of the wind speed ΔSWS between SMOS and SMAP as a function of SMOS SWS across-track distance. The mean theoretical wind speed error provided in the NRT product is shown in magenta. The theoretical error +1.2 m/s is shown in dashed black. Left: old processor version 110. Right: new processor version 300.

5. With the new processor, **the land contamination seems highly reduced for the retrieved SWS at distances to coasts larger than 250 km** (unbiased with constant RMSD of ~2 m/s for all QLs). Close to coasts (< 250 kms), the bias and RMSD are

also significantly reduced (see Figure 6). However, close to coasts, SMOS minus SMAP differences remain high but with a reverse bias pattern (SMOS winds are now too small with respect SMAP on average while it was the reverse situation with the old processor).

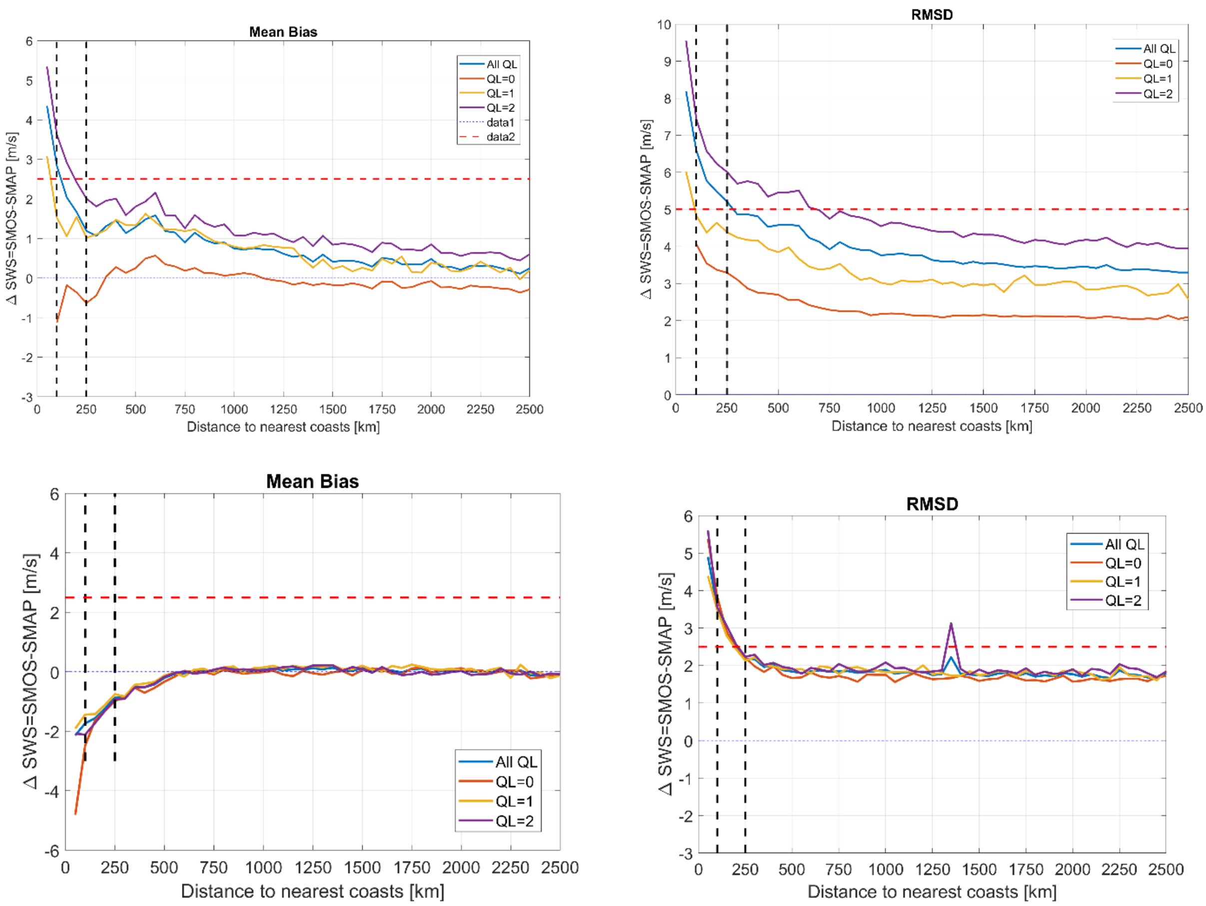

Figure 6 : Mean (left) and RMSD (right) of the ΔSWS (SMOS-SMAP) as a function of distance to coasts. The color indicate SMOS QL levels. Top: old processor version 110. Bottom: new processor version 300

6. As found **the percentage of absolute SMOS-SMAP SWS data greater than 2.5 m/s significantly reduced with the new processor**, mostly found in the coastal domain or sea-ice borders (see Figure 7).

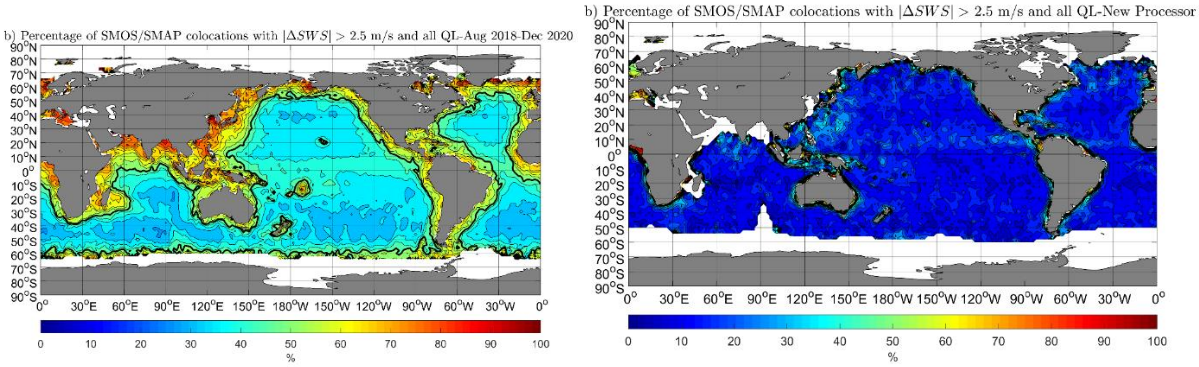

Figure 7 : Percentage of match-up co-localized points in 2°x2° boxes between SMOS NRT and SMAP wind speeds for which the wind speed difference between the co-localized data |∆SWS| exceed 2.5 m/s. The thick black contour is at 50%. (left) Old processor version 110 (right) New processor version 300.

7. with the new processor the **biases and RMSD have been reduced in all oceanic regions and for all QL values, except in the Arctic** (see Figure 8 and Figure 9)**.** Improvements are clearly evidenced for SWS retrievals with QL=1 and QL=2 in all regions. The regions are defined as follows:

   - Reg 1 : Global ocean
   - Reg 2 : North Atlantic
   - Reg 3 : South Atlantic
   - Reg 4 : North-East Pacific
   - Reg 5 : North-West Pacific
   - Reg 6 : South Pacific
   - Reg 7 : North Indian Ocean
   - Reg 8 : South Indian Ocean
   - Reg 9 : Arctic Ocean
   - Reg 10 : Roaring forties & furies fifties
   - Reg 11 : Near coasts global region

   The spatial extent of each of these regions is available in netcdf format here.

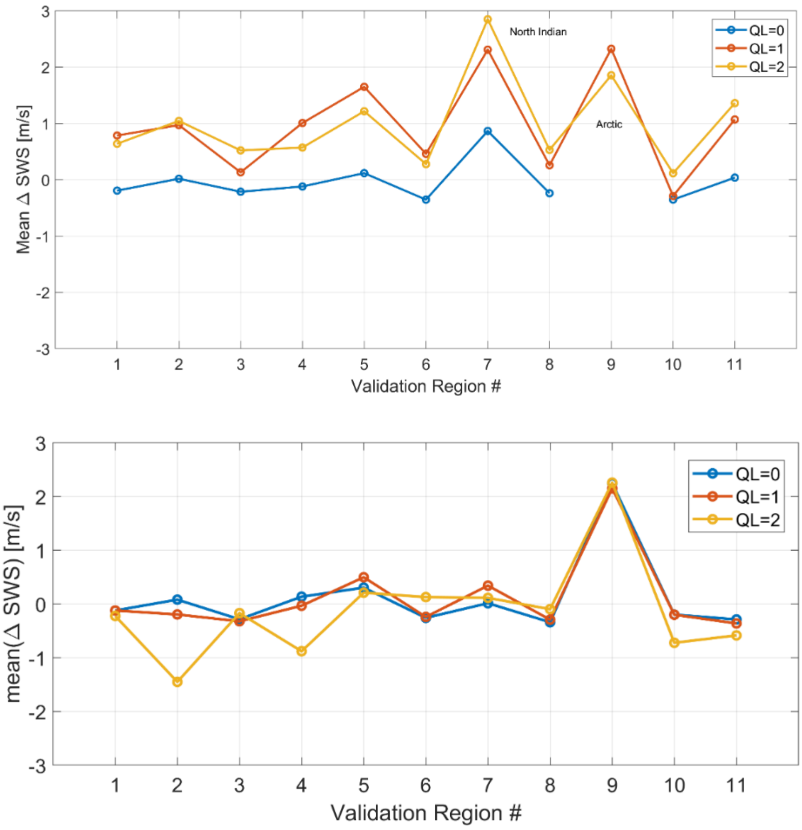

Figure 8 : Mean bias between collocated SMOS NRT winds and SMAP winds for each validation region. The results are split as a function of the SMOS NRT wind data quality (blue is QL=0, red is QL=1 and yellow is QL=2). (top) Old processor version 110 (bottom) New processor version 300.

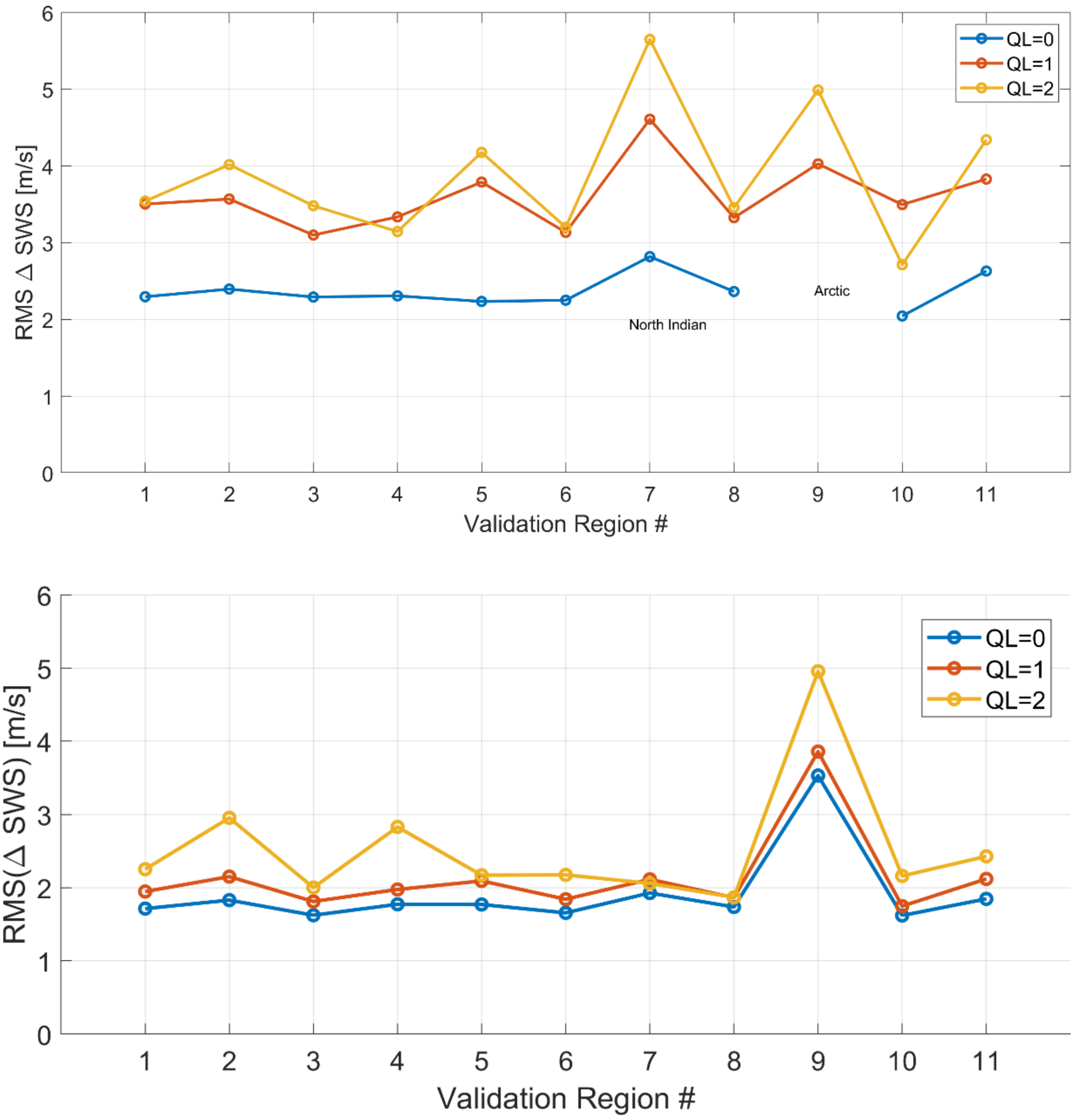

Figure 9 : RMSD between collocated SMOS NRT winds and SMAP winds for each validation region. The results are split as a function of the SMOS NRT wind data quality (blue is QL=0, red is QL=1 and yellow is QL=2). results are split as a function of the SMOS NRT wind data quality (blue is QL=0, red is QL=1 and yellow is QL=2). (top) Old processor version 110 (bottom) New processor version 300.

The wind radii produced from SMOS NRT L2 wind processor have been **compared to the Tropical cyclone best track** re-analysis data over 2015. The **RMSD between SMOS NRT wind radii and Best track data are 31, 26, and 22 nautical mile for the gale (34 kt), storm (50 kt), and hurricane (64 kt) radii**, respectively. The SMOS NRT values are below the best track uncertainties from satellite-only measurements (i.e., no aircraft data) and regardless of storm intensity.

2.8. Recommandations

We strongly advise users to consider SMOS NRT wind data with caution.

- when the distance to nearest coast is less than 250 km,
- in the Arctic ocean,
- in oceanic regions with highly variable surface salinity (Large River plumes, boundary currents, etc..)
- when the absolute across-track distance from the central part of the swath exceed 400 km,
- when the data quality level is equal to 2.
- when the retrieved wind speed is less than 5 m/s (the data are mostly forced to follow the first guess, which is given by ECMWF forecasts)

For operations, we therefore advise to use only SMOS NRT wind QL equal to 0 and 1.

2. SMOS NRT Wind Products Access

The SMOS NRT wind products can be accessed in two manners using either the Ifremer or ESA/SMOS dissemination services:

2.1. Dissemination service at Ifremer

The complete archive of generated SMOS Wind Service products is accessible to the user community online, through FTP and HTTPS. While FTP is still very popular, it is also being banned now by many agencies. The complementary HTTPS access service is therefore proposed to users providing to the exact same product archive, through the same credentials.

The credentials to access the data will be obtained from a simple registration web form hosted at Ifremer. They will be returned automatically to the user once he has completed the registration process.

The **FTP service** uses the following credentials.

Url	ftp://eftp1.ifremer.fr
Path	/smos-wind
Login	s031c63
Password	<to be obtained at https://forms.ifremer.fr/lops-siam/smos-wind-data-access/>

The **HTTP service** uses the same credentials:

Url	https://smos-wind.ifremer.fr
Path	/
Login	s031c63
Password	<to be obtained at https://forms.ifremer.fr/lops-siam/smos-wind-data-access/>

2.2. ESA SMOS Dissemination Service

The SMOS NRT wind products are available on the SMOS Data Dissemination Server (https://smos-diss.eo.esa.int).
Data is organised into collections accessible via a web interface and via FTP.
A Simple Catalogue allows for data navigation and selection by data type and acquisition date.
In order to download files, users must be logged in with an ESA EO Signed In account (to create one please follow this link: https://eoiam-idp.eo.esa.int).

3. Access to SMOS NRT Wind Product Documentation

The three following documents are available to provide users with necessary information for proper utilization of the SMOS Wind Data Service products.

These documents are available from:

http://www.smosstorm.org/Document-tools/SMOS-Wind-Data-Service-Documentation

or from:

https://earth.esa.int/eogateway/catalog/smos-nrt-l2-swath-wind-speed

Document Name	Content
SMOS Wind Data Service Readme First Note	A summary of the validation results The way to access the data through both ESA/SMOS dissemination portal and Ifremer FTP/HTTP The way to access SMOS wind documentation
SMOS Wind Data Service Algorithm Theoretical Basis Document	Describe the Algorithms used to generate: 1. the SMOS Level2 NRT wind products 2. the NRT wind radii estimates from the SMOS wind L2 swath data intercepts with Tropical Cyclones 3. the SMOS Level 3 wind daily products
SMOS Wind Data Service Product Description Document	Describes the 3 data products generated by the ESA/SMOS Wind Data Service operated by IFREMER/OceanDataLab

4. Scientific publications

The following is a list of scientific papers relevant for the SMOS NRT wind product.

Title	Code	Date
Kerr Yann H and coauthors. The SMOS Mission: New Tool for Monitoring Key Elements of the Global Water Cycle.	Proceedings of the IEEE, 98(5), 666-687. http://doi.org/10.1109/JPROC.2010.2043032	2010
Mecklenburg S.and coauthors. ESA's Soil Moisture and Ocean Salinity mission: From science to operational applications.	Remote Sensing Of Environment, 180, 3-18. http://doi.org/10.1016/j.rse.2015.12.025.	2016
SMOS satellite L-band radiometer: A new capability for ocean surface remote sensing in hurricanes.	Journal Of Geophysical Research-oceans , 117	2012
A revised L-band radio-brightness sensitivity to extreme winds under Tropical Cyclones: the five year SMOSstorm database.	Remote Sensing of Environment 180 (2016)274–291 n/a 10.04.2016	2016
A new generation of Tropical Cyclone Size measurements from space.	Bulletin of the American Meteorological Society.	2017
Uhlhorn and co-authors. Hurricane surface wind measurements from an operational stepped frequency microwave radiometer,	*Mon. Weather Rev.*, **135**, 3070–3085, doi:10.1175/MWR3454.1.	2007
Powell M.D. (2010), Near-surface based, airborne, and satellite observations of tropical cyclones, J.C.L. Chan, J.D. Kepert.	(Eds.), Global perspectives on tropical cyclones: From science to mitigation (2nd ed.), World Scientific Publishing Company, pp. 177–199.	2010
Yin, X., J. Boutin, E. Dinnat, Q. Song, and A. Martin, 2016. Roughness and foam signature on smos-miras brightness temperatures: A semi-theoretical approach.	Remote sensing of environment, 180:221–233, 471.	2016
Oliva R and co-authors. Status of Radio Frequency Interference (RFI) in the 1400–1427MHz passive band based on six years of SMOS mission.	Remote Sensing Of Environment, 180, 64-75. http://doi.org/10.1016/j.rse.2016.01.013	2016
Boutin, J., and co-authors. Satellite and in situ salinity: understanding nearsurface stratification and sub-footprint variability.	Bull. Am. Meteorol. Soc. 97 (10). http://dx.doi.org/10.1175/BAMS-D-15-00032.1.	2016
Price, J. F. Upper ocean response to a hurricane.	Journal of Physical Oceanography 11, 153–175.	1981
Jourdain, N.C and co-authors Observation-Based Estimates of Surface Cooling Inhibition by Heavy Rainfall under Tropical Cyclones.	Journal of Physical Oceanography 43:1, 205-221.	2013
Wentz, F., The effect of clouds and rain on the Aquarius salinity retrieval.	Remote Sensing Systems Tech. Memo. 3031805, 14 pp. [Available online at http://images.remss.com/papers/aquarius/rain_effect_on_salinity.pdf.]	2005
SMAP L-Band Passive Microwave Observations Of Ocean Surface Wind During Severe Storms.	Ieee Transactions On Geoscience And Remote Sensing , 54(12), 7339-7350	2016
Capability of the SMAP Mission to Measure Ocean Surface Winds in Storms.	Bulletin of the American Meteorological Society.	2017
Using routinely available information to estimate tropical cyclone wind structure.	Mon. Wea. Rev., 144:4, 1233-1247.	2016

"International Workshop on Measuring High Wind Speeds over the Ocean"-Proceedings.	SMOSSTORMEvolution_WKP_D160	2017
SMOS L2 OS Algorithm Theoretical Baseline Document.	SO-TN-ARG-GS-0007_L2OS-ATBD	2016
Kudryavtsev V.,P. Golubkin, B. Chapron, A simplified wave enhancement criterion for moving extreme events.	Journal of Geophysical Research, Oceans, 120, http://dx.doi.org/10.1002/2015JC011284.	2015
Sampson, C. R., and A. J. Schrader, The Automated Tropical Cyclone Forecasting System (version 3.2).	Bull. Amer. Meteor. Soc., 81, 1231–1240	2000
Boutin J. and co-authors. New SMOS Sea Surface Salinity with reduced systematic errors and improved variability.	Remote Sensing Of Environment, 214, 115-134.	2018
Bourassa, M. and co-authors. Remotely Sensed Winds and Wind Stresses for Marine Forecasting and Ocean Modeling	Frontiers In Marine Science , 6(443), 28p.	2019